

Jan Hricák, [jan.hricak@fsv.cvut.cz](mailto:jan.hricak@fsv.cvut.cz)

WG3 - Michal Jandera, [michal.jandera@fsv.cvut.cz](mailto:michal.jandera@fsv.cvut.cz)

WG2 – František Wald, [wald@fsv.cvut.cz](mailto:wald@fsv.cvut.cz)

## 7 LOCAL BUCKLING OF STEEL CLASS 4 SECTION BEAMS

### Summary

A significant progress in fire engineering research was made in the last decade. This resulted in more precise structural fire design and higher reliability of steel structures. However, for design of very slender sections (Class 4 cross-sections according to the Eurocode 3), where elevated temperature affects also behaviour of elements subjected to local buckling, no wide research was published. Therefore, the benchmark shows numerical simulations of slender open section beam at elevated temperature where the bending resistance affected only by local instabilities was reached.

### 7.1 INTRODUCTION

A common practice in recent years is the design of structures not just for the standard design situation but also in case of extreme events such as fire. Design of steel structures in fire was also supported by European design standards (EN 1993-1-2:2005). For the slender sections, as described here, the design is more complex because of the possible local instabilities. This leads to calculation of effective section properties (EN 1993-1-5:2006) which makes the structural design more difficult compared to stocky sections. Considering also the fact of very small background research for the slender sections at elevated temperature, the possibility of using FE model may be therefore advantageous.

The focus of the benchmark studies is to carry out numerical simulations with Class 4 open I – section beams. The load capacity was reached by pure bending on a simple supported beam loaded symmetrically by two concentrated forces. The mid span of the beam was therefore loaded by uniform bending moment with no shear force. The lateral restraint was considered in such way to avoid lateral torsional buckling (see Fig. 7.1). Four cases with two types of cross-section were simulated at two different temperatures. The selected sections and load set-up results from real tests carried out in the framework of RFCS project FIDESC4.

The simulation assumed steady state test where the temperature is constant during the test and the load increases. In this case, load was assumed as displacement controlled. Therefore, also the descending branch of the load-deflection diagram was recorded. For both section types (Fig. 7.2), only the central part of the beam was heated. The temperatures of 450 °C and 650 °C were used in the tests.

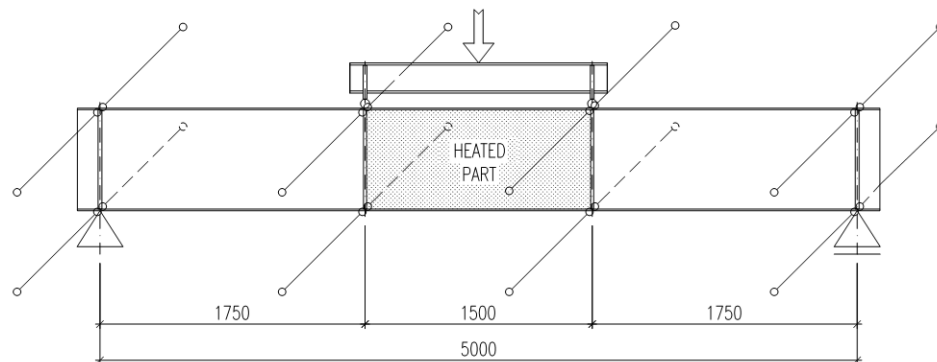


Fig. 7.1 Simulated beam

The section A (IS 680/250/12/4) had the web of Class 4 and the flanges of Class 3, if classified according to the current EN 1993-1-1:2005 (Fig. 7.2 a). The section B (IS 846/300/8/5) had both the web and flanges of Class 4 (Fig. 7.2 b).

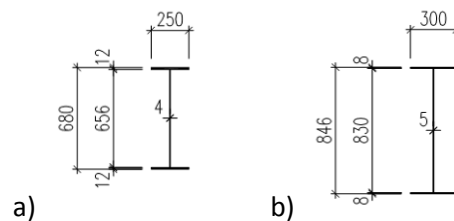


Fig. 7.2 Cross sections used in the simulation:

a) section A, b) section B

## 7.2 FE MODEL

The numerical part includes description of a FE numerical model. It was made in general FE software ABAQUS. The detailed description is given.

### 7.2.1 Mesh and elements

For the modeling of thin-walled elements, it is advantageous to use shell elements. These elements are suitable for modelling of plates of the slenderness more than 10 (width to thickness ration) which was satisfied for all parts of the selected profiles. Element S4 (Fig. 7.3) was finally used based on a comparative study of the shell elements.

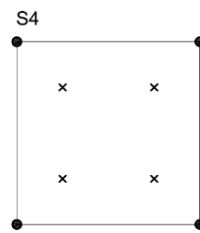


Fig. 7.3 Shell element S4

The shell element S4 has four nodes with six degrees of freedom (three displacements and three rotations), linear approximation and full integration (4 integration points on the surface of the element). It can be used in the calculation of large deformations and large rotations. For each model of the beam, there were 200 nodes used in the direction of the web length. Across the web width 16 elements were used, whereas the flanges were represented by 6 elements in their width. The structural mesh is shown in Fig 7.6.

### 7.2.2 Geometrical imperfections

Local imperfections were introduced by the shape of the first elastic buckling eigenmode (Fig. 7.4). The amplitude in the benchmark example was considered by the value given in the design code EN 1993-1-5. The imperfections of the flange was  $2 \times 1/200$  times the length of the outstanding flange and amplitude for the web was  $1/200$  of web height.

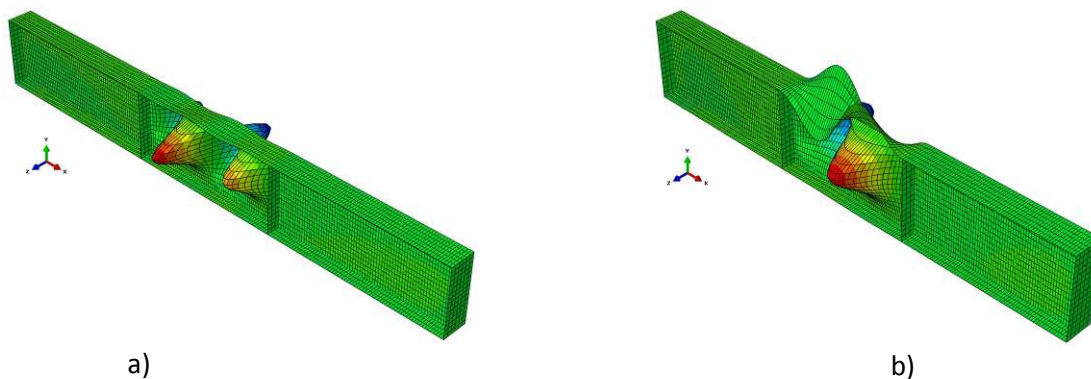


Fig. 7.4 The first elastic buckling eigenmode shape, a) simulation 1 and 2, b) simulation 3 and 4

The residual stresses in the section were not included in the study, despite their influence on the load capacity may be not negligible.

### 7.2.3 Material modeling

Mechanical properties were defined for structural steel S355 (yield strength  $f_y = 355$  MPa, modulus of elasticity  $E = 210$  GPa, Poisson's ratio  $\nu = 0.3$ ). Mechanical properties at high temperature were obtained using the reduction factors dependent on temperature as given by EN 1993-1-2. Material behaviour at high temperature was defined by the elastic-plastic non-linear stress-strain relationship (Fig. 7.5).

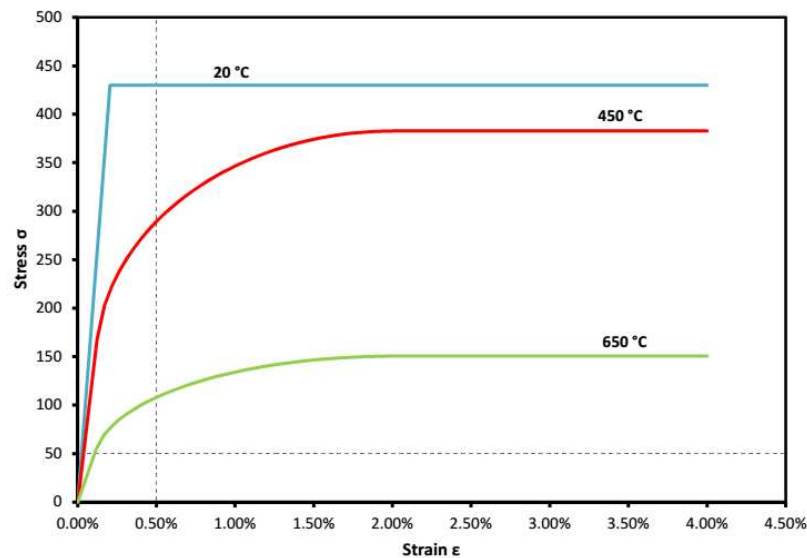


Fig. 7.5 Stress–strain relationship for steel S 355 depending on the temperature

### 7.2.4 Boundary conditions and loading

For the simulation, boundary conditions were defined according to the Figure X.1. All nodes of the lower flange support on one side (point "a" in Fig. 6) were restricted to the vertical direction and the direction of the beam axis. The other side supported all nodes across the flange width in the vertical direction only (node "d"). The hinged support was chosen on the left side of the model (point "a") and the roller on the right-hand side (point "d"), see Fig. 7.6. On the left side, shift in the direction of the  $x$ ,  $y$ ,  $z$  axis and the rotation about the  $x$  axis were blocked, the rotation about the  $z$  axis was possible. On the right-hand side, the boundary conditions were the same except the free horizontal movement in the direction of the beam axis  $x$ . For the section where the load was applied (points "b", "c"), lateral restraint is considered (in the direction of the  $z$  axis).

The static structural analyses (load–displacement analyses) were performed to predict the load–deflection behaviour of the steel beams. Regarding the application of load, two concentrated loads were defined incrementally by means of equivalent displacements to record also the descending branch of the diagram. Vertical displacements were applied at the top flange at the two points (Fig. 7.1) and the load step increments were varied in order to solve potential numerical problems. The region between

the two loading points (L = 1500 mm) is the part decisive for the member resistance where uniform bending moment acts. Load points are also shown in Fig. 7.6.

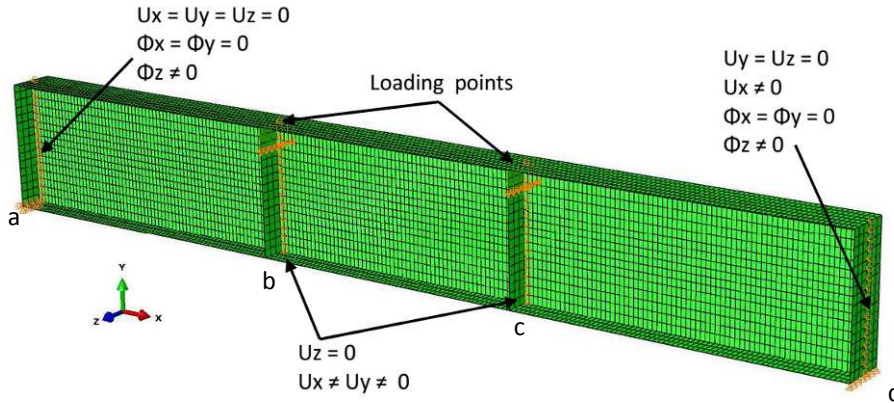


Fig. 7.6 Loading and boundary conditions for beam model

### 7.2.5 Temperature distribution in numerical model

Each beam was modelled at constant temperature. The side parts between the support and the load point were considered at room temperature (20°C) whereas the central part at elevated temperature as specified in Table 7.1 (Fig. 7.7). This simulated tests where only the central part was heated by ceramic pads with rheostatic wires.

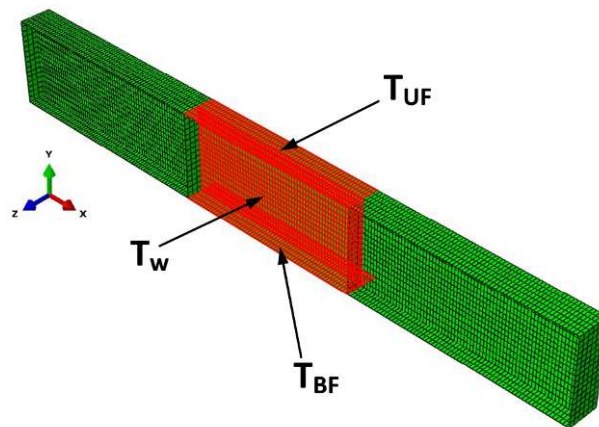


Fig. 7.7 Temperature distribution in numerical modeling

Tab 7.1 Temperatures for the simulations

	A (IS 680/250/4/12)		B (IS 846/300/5/8)	
Simulation	1	2	3	4
Temp. [°C]	450	650	450	650

### 7.3 RESULTS OF THE NUMERICAL SIMULATION

The results obtained by the numerical simulations are presented in this section. Failure mode of numerical model is also given in the figures.

#### 7.3.1 Simulation 1 and Simulation 2 (IS 680/250/4/12)

The following figures (Fig. 7.8 and 7.9) show the deformed shape of the central heated part and load-deflection diagram.

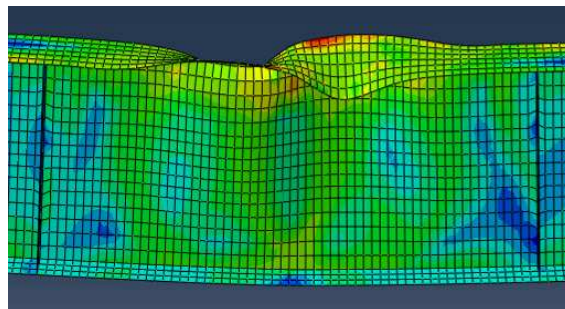


Fig. 7.8 Central part of the beam for the simulation 1 and 2

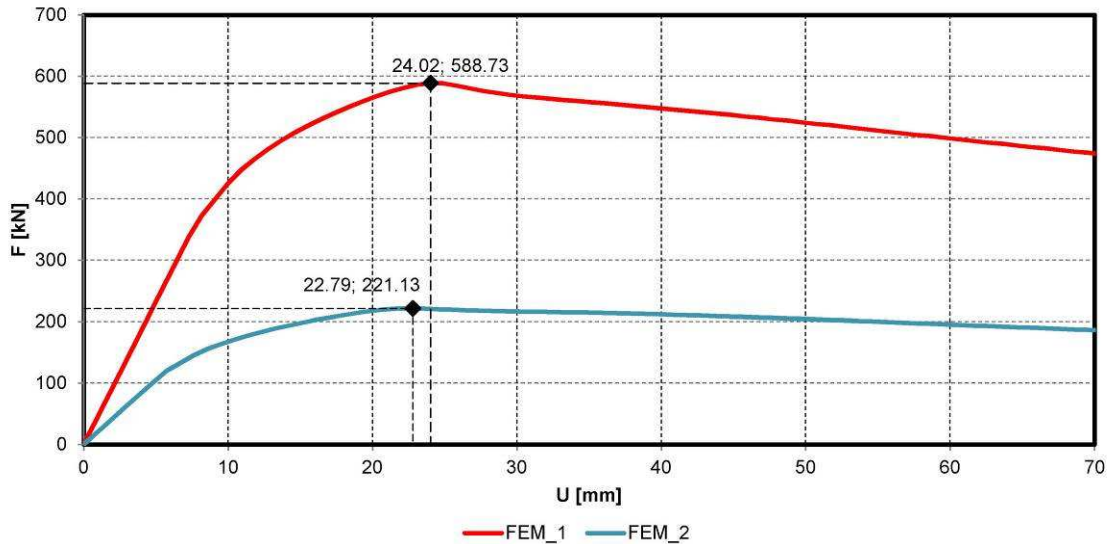


Fig. 7.9 Load-deflection diagram for simulation 1 and 2

#### 7.3.2 Simulation 3 and Simulation 4 (IS 846/300/5/8)

Figures 7.10 and 7.11 show the failure shape and load-deflection diagram for the numerical simulation 3 and 4.

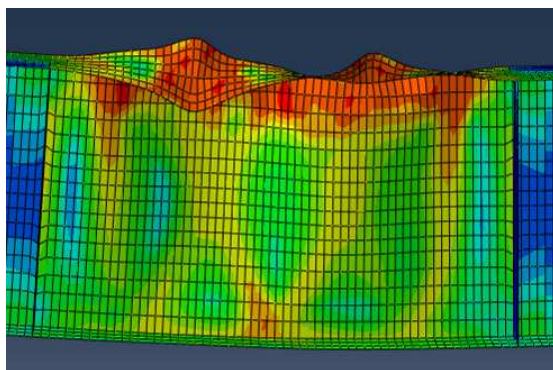


Fig. 7.10 Central part of the beam for simulation 3 and 4

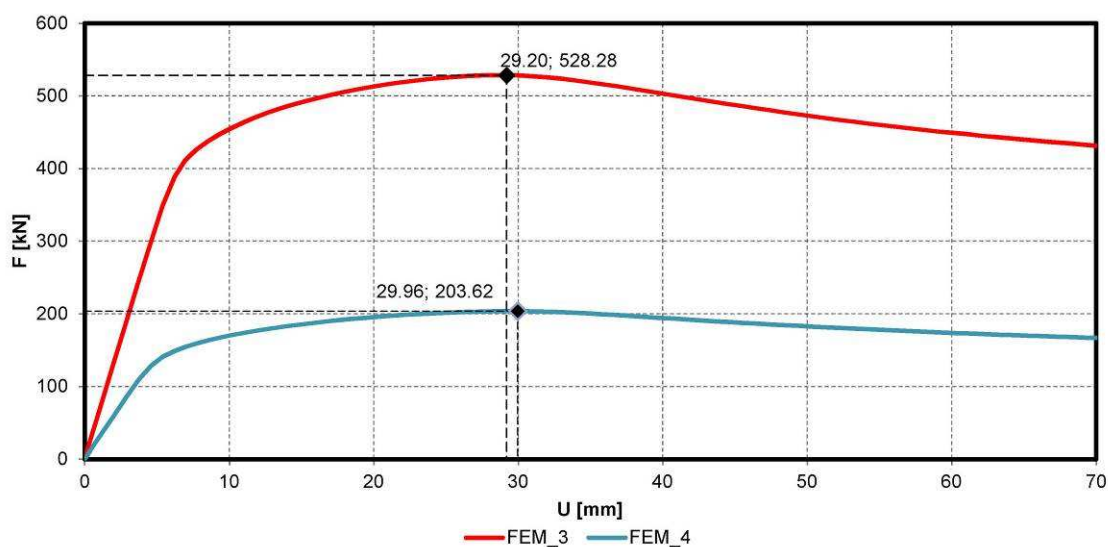


Fig. 7.11 Load-deflection diagram for simulation 3 and 4

The ultimate load capacity given in means of the maximum load applied is listed in the following table (Tab. 7.2).

Tab. 7.2 Load capacity of the simulated beams

Simulation	Cross-section	Max. load [kN]
		FEM
1	A1 (IS 680/250/4/12)	588.73
2	A2 (IS 680/250/4/12)	221.13
3	B1 (IS 846/300/5/8)	528.28
4	B2 (IS 846/300/5/8)	203.62

## 7.4 CONCLUSIONS

The benchmark example shows a FE numerical model of Class 4 open section beams with no influence of lateral-torsional buckling. Two types of the sections were considered, both at two levels of temperature. The example shows the details of the model including boundary conditions, imperfections etc. As a result, the load-deflection curves of steady state test simulation as well as the failure modes are given.

### References

- ABAQUS: Analysis user's manual, Volumes I-IV, version 6.10. (2010). Hibbitt, Karlsson & Sorenses, Inc., Providence, R.I, USA.
- CEN. Eurocode 3: design of steel structures, part 1.1: general rules and rules for buildings (EN 1993-1-1:2005). Brussels, 2005
- CEN. Eurocode 3: design of steel structures, part 1.2: general rules—structural fire design (EN 1993-1-2:2005). Brussels, 2005
- CEN. Eurocode 3: design of steel structures, part 1.5: plated structural elements (EN 1993-1-5:2006). Brussels, 2006.